Recent Shift in Eurasian Boreal Forest Greening Response May be Associated with Warmer and Drier Summers

Author list: Wolfgang Buermann, Bikash Parida, Martin Jung, Glen M. MacDonald, Compton J. Tucker, and Markus Reichstein

AUXILIARY MATERIAL

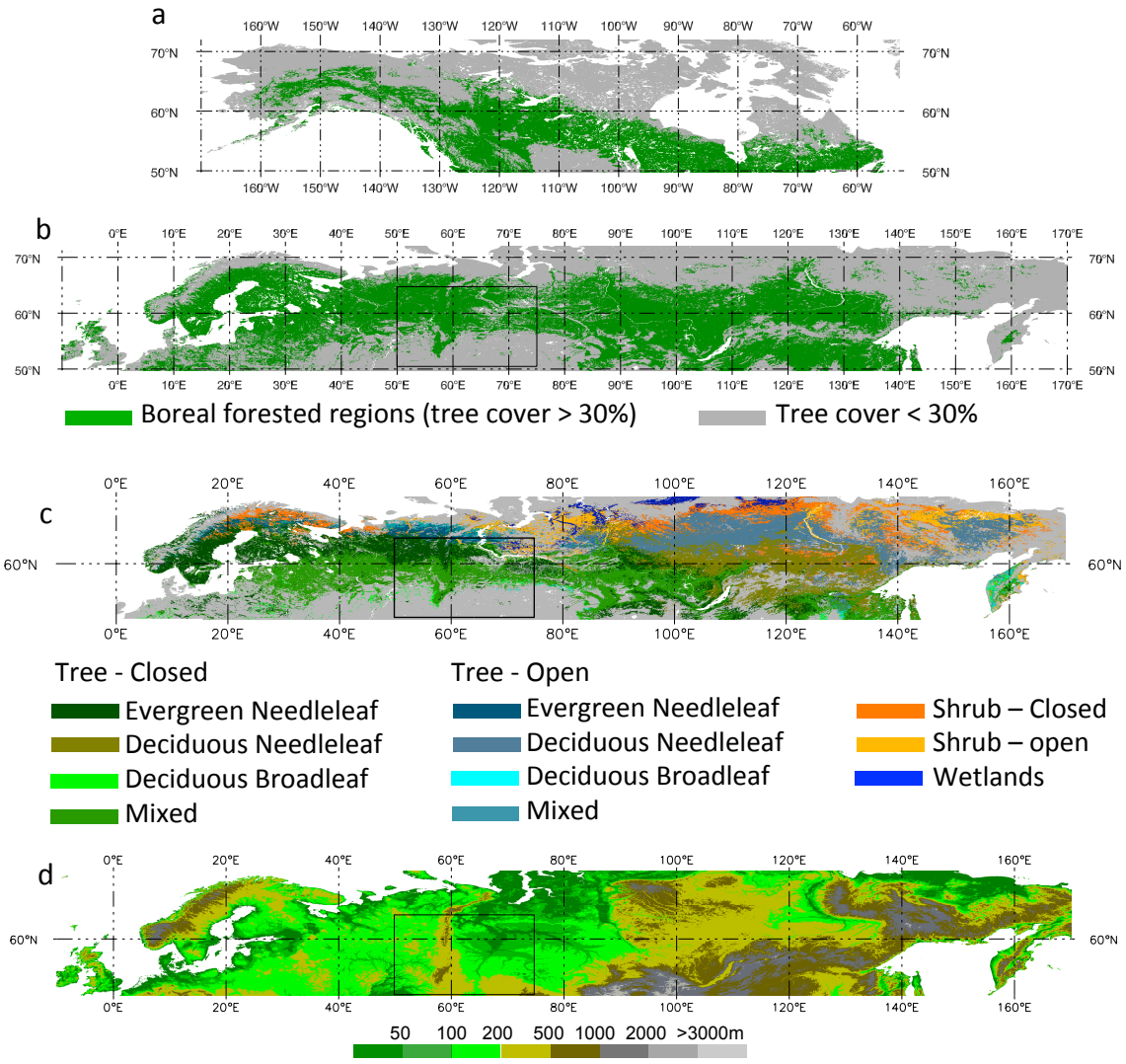

Figure S1: Boreal forest study region, EA land cover and topography. Panels (a) and (b) show boreal forested regions, defined as all areas in the latitude band from 50°N to 70°N having aggregated tree cover > 30% based in the (500m) 2001 MODIS vegetation continuous fields (S1). Panel (c) depicts land cover based on the Northern Eurasian Land Cover (NELC) Database (S2), and in (d) a elevation map based on Shuttle Radar Topography Mission (SRTM) data is shown. In (b), (c), and (d) the Ural focus region (50°E-75°E and 50°N-65°N) is outlined (rectangle).

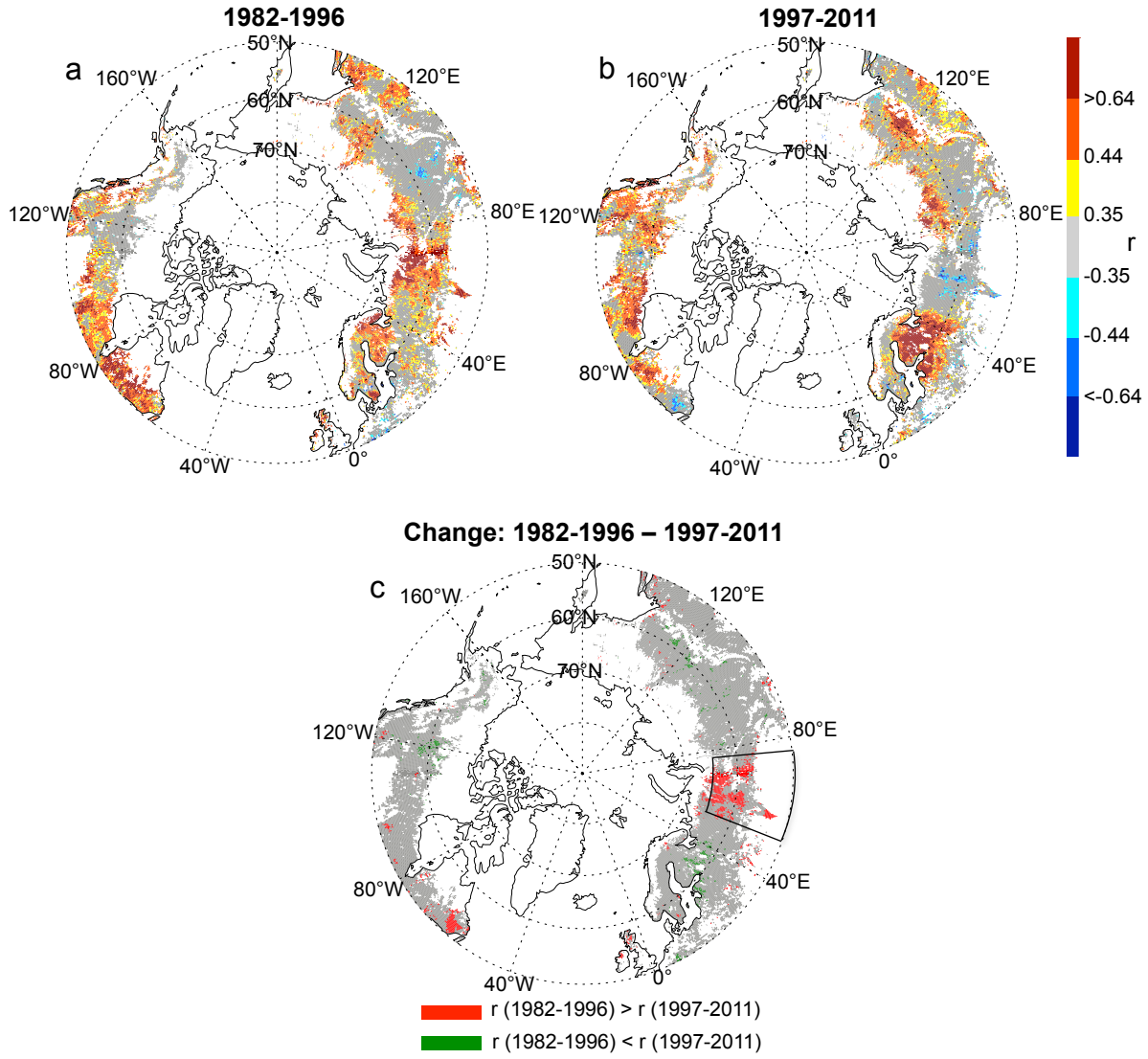

Figure S2: Interannual relationships between summer surface temperature and vegetation greenness across boreal forests. Maps depict grid cell correlations between annual summer (JJA) temperature and NDVI for the periods (a) 1982-1996 and (b) 1997-2011, respectively, as well as (c) statistically significant ($P < 0.05$) correlation changes between these two periods. Here, linear trends (determined through least square regression) based on the two target periods were removed in the original data prior to correlations (S3). In (c), the Ural focus region is highlighted. The absolute r-value categories shown correspond to $P < 0.2$ (r = 0.35), $P < 0.1$ (r = 0.44) and $P < 0.01$ (r = 0.64) significance levels.

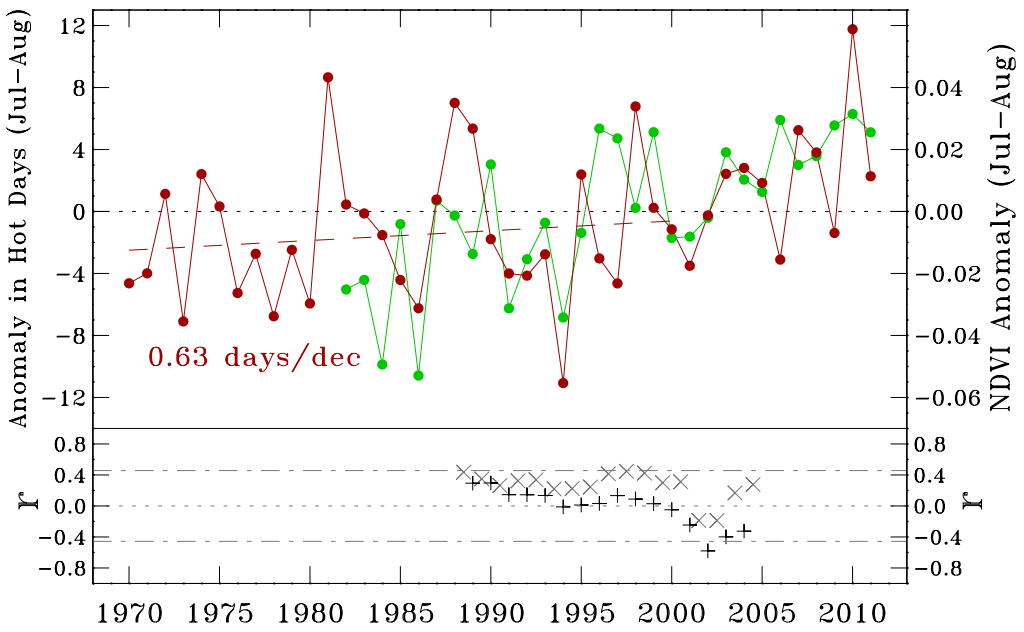

Figure S3: Temporal changes in peak summer boreal forest greenness and number of hot days for the Ural focus region. For peak NH summer (Jul-Aug), annual anomalies in spatially averaged NDVI (green) are plotted alongside anomalies in the number of days exhibiting daily maximum temperatures above 25°C (dark red), a threshold that may signal heat stress for boreal trees (S4). All anomalies are relative to the period 1982-2011, and the trend in number of hot days (dashed red line) corresponds to the period 1970-2000. Daily maximum temperature records stem from NCEP reanalysis (S5). Here, the Ural focus region encompasses all forested areas within 50°E-75°E and 50°N-65°N (unlike in Fig. 2 in main ms) owing to the relatively coarse NCEP reanalysis data (~2° spatial resolution). The lower panel depicts moving window correlations based on 14-yr periods between original data (grey crosses) and after removing a trend within each time slice via first differences (pluses), whereby the corresponding correlation are plotted in the middle (year 7) of each interval. Correlations above/below the horizontal grey dashed-dotted lines are statistically significant at the 90% level (absolute r $\geq$ 0.46).

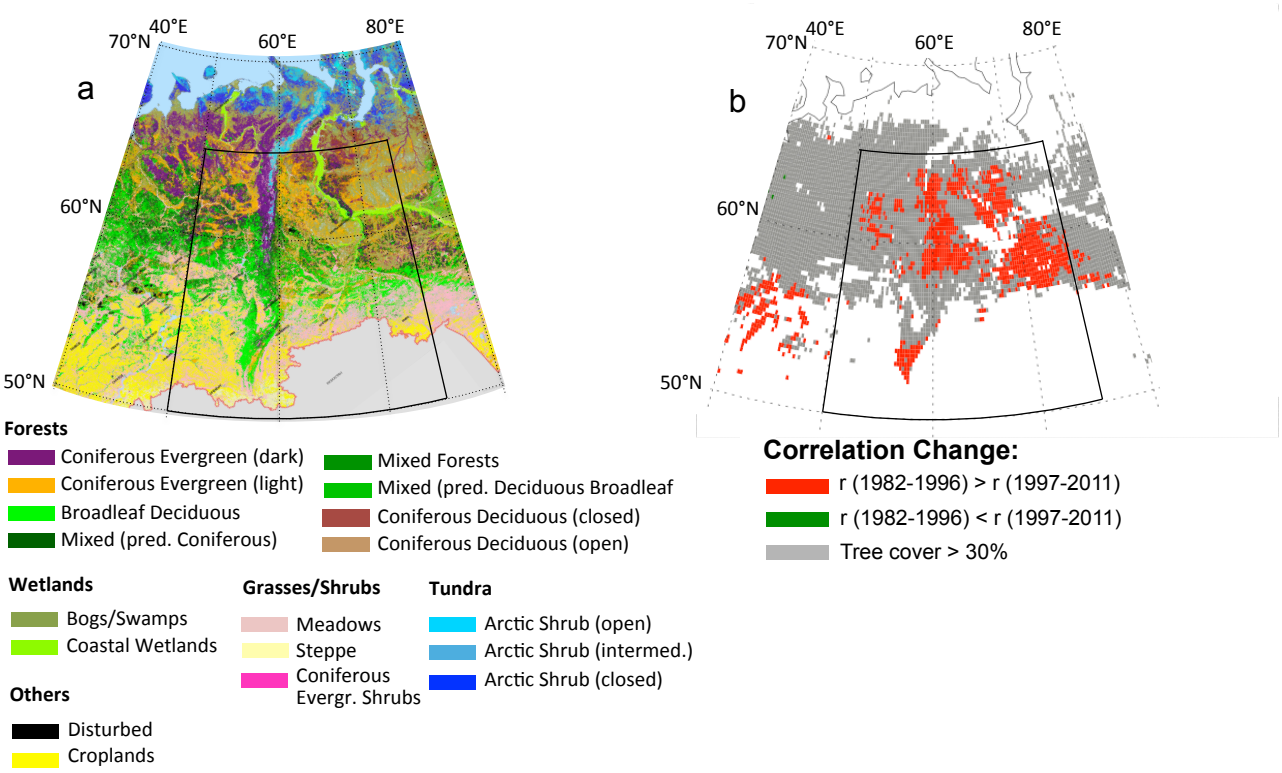

Figure S4: Comparison of correlation change pattern with high-resolution land cover in the Ural focus region (Part 1). Maps depict (a) high-resolution Russian land cover and (b) statistically significant changes ($P < 0.05$) in grid cell correlations between annual summer (JJA) temperature and NDVI for the periods (a) 1982-1996 and (b) 1997-2011, respectively. Panel (b) represents a close up of Fig. 1c in the original manuscript and in panels (a) and (b) the Ural focus region is outlined. The high-resolution (~250m) Russian land cover map shown was produced by the Russian Academy of Sciences' Space Research Institute based on MODIS data from 2010 and a locally-adaptive algorithm for supervised classification.

(see *http://smiswww.iki.rssi.ru/* for detailed description and map file).

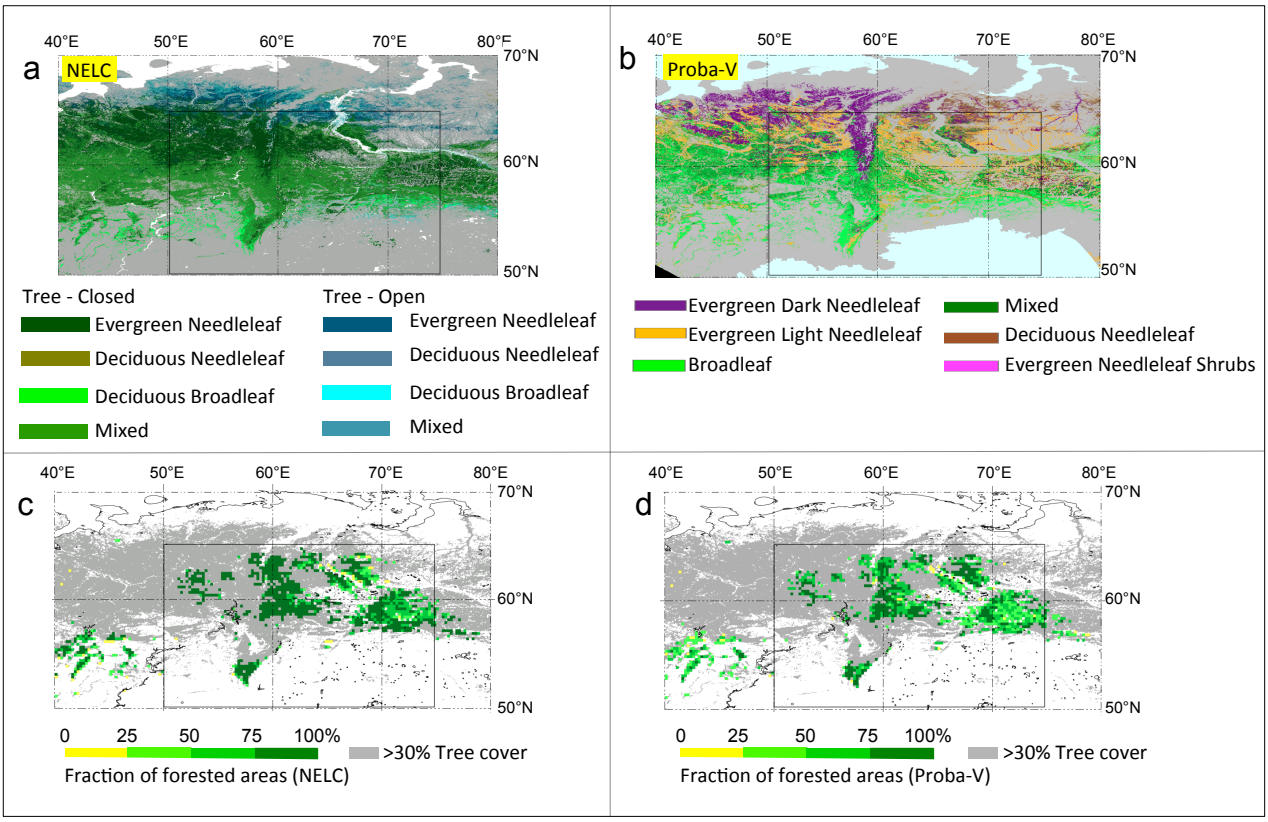

Figure S5: Comparison of correlation change pattern with high-resolution land cover in the Ural focus region (Part 2). Maps depict (a) high-resolution (~500m) forest cover based on NELC (S2) and (b) high-resolution (345m) Russian forest cover from the Proba-V-TerraNorte project. In (c) and (d), maps show the fraction of forests within the coarser (~25km) correlation change pattern (defined as in Fig. 1c in original ms) based on the NELC (c) and Proba-V-TerraNorte (d) classification, respectively. In all panels, the Ural focus region is outlined. The Proba-V TerraNorte forest classification is based on MODIS data from 2010 and a locally-adaptive algorithm for supervised classification (see *http://smiswww.iki.rssi.ru/* for detailed description and map file).

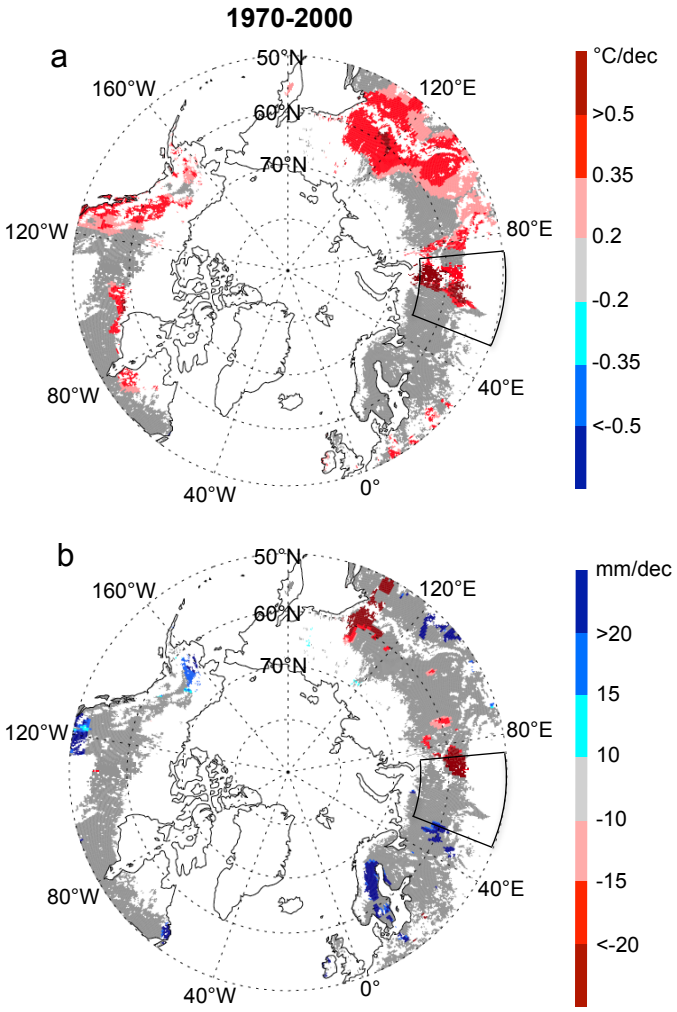

Figure S6: Long-term trends in summer surface temperature and precipitation across boreal forests. Maps depict decadal trends in summer (JJA) temperature (a) and precipitation (b) for the period 1970-2000. Trends are based on linear least squares regression and here only those trends are shown that are statistically significant ($P < 0.1$). Original high-resolution climate data stem from the Climatic Research Unit (CRU) (S6).

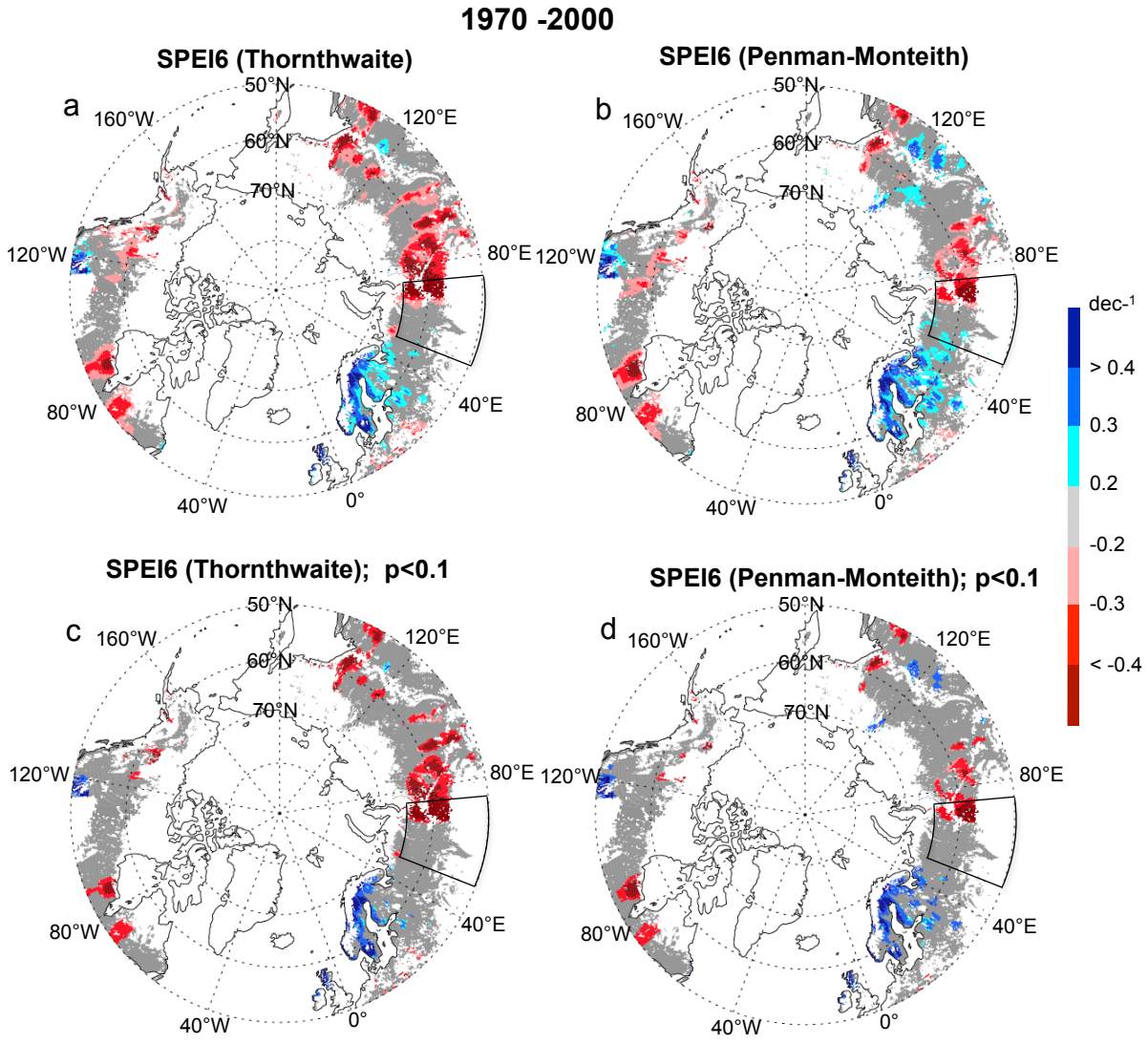

Figure S7: Decadal trends in summer climatic water deficit across boreal forests. Maps depict decadal trends in summer (JJA) SPEI6 without statistical filter (a,b) and with filter ($P < 0.1$) (c,d) for the period 1970-2000. Trends are based on linear least squares regression. Climate data were obtained from the Climatic Research Unit (CRU) (S6). In panels (a,c) SPEI6 were calculated with PET based on Thornthwaite, whereas in (b,d) PET is based on Penman –Monteith (see Data and Methods in main ms).

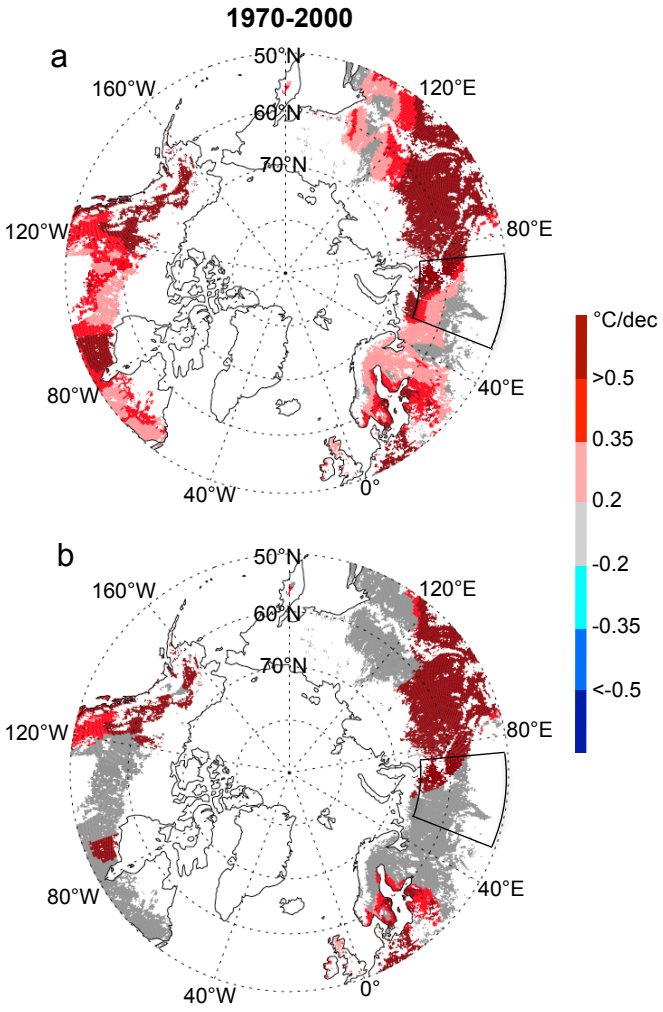

Figure S8: Long-term trends in spring surface temperature across boreal forests. Maps depict decadal trends in spring (MAM) temperature without statistical filter (a) and with filter ($P < 0.1$) (b) for the period 1970-2000. Trends are based on linear least squares regression. Original climate data were obtained from the Climatic Research Unit (CRU) (S6).

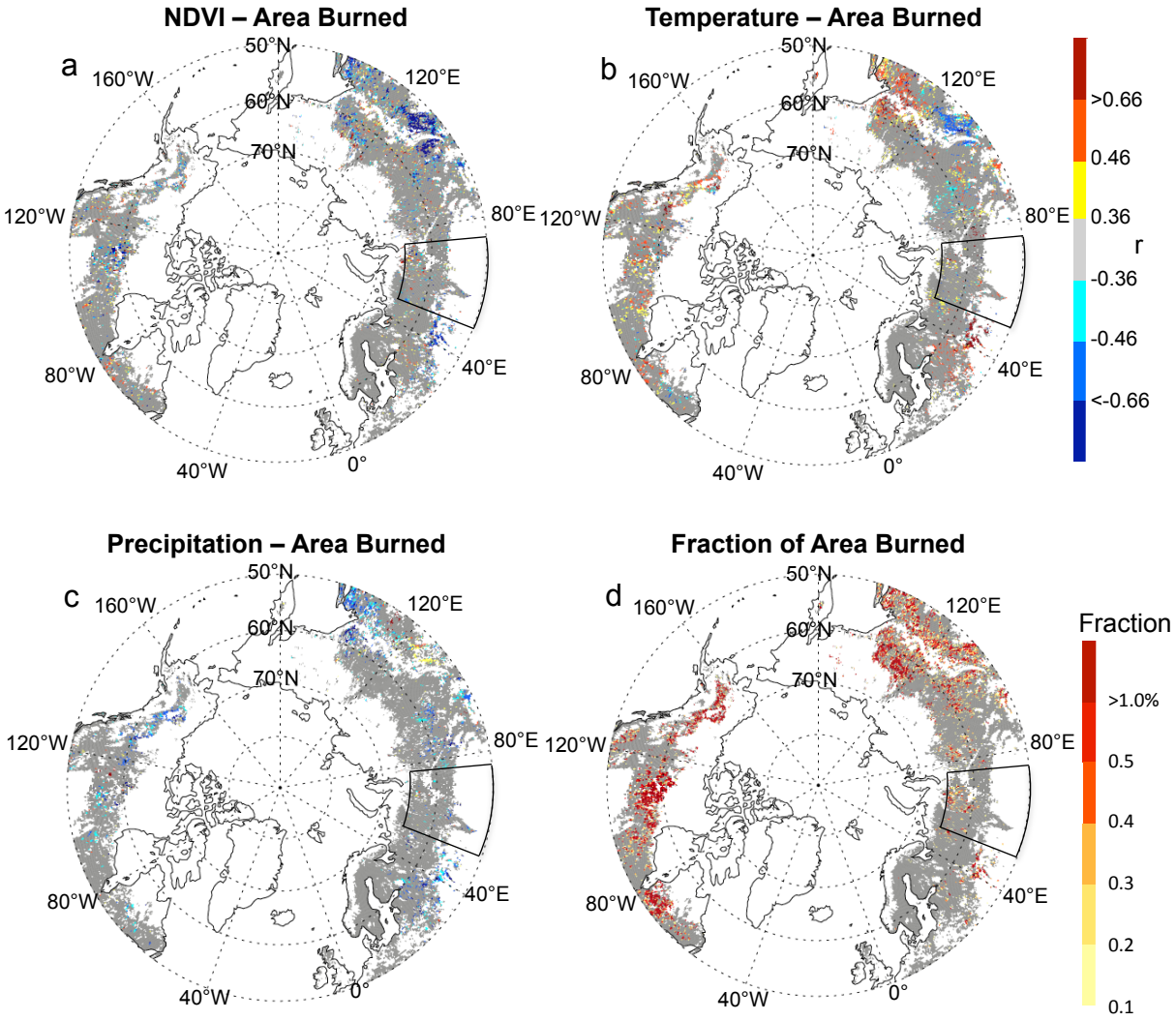

Figure S9: Interannual relationships between area burned and NDVI as well as climate across boreal forests during NH summer. Grid cell correlations between annual NH summer (JJA) area burned (S7) and (a) NDVI, (b) temperature, and (c) precipitation for the 1997-2011 period for which burned area and NDVI data were available. In (d), the summer (JJA) climatology of the fraction of burned area within a grid cell is shown (based on 1997-2011). Original data were detrended prior correlations through the first differences method. In all panels, the Ural focus region is outlined .The absolute r-value categories shown correspond to $P < 0.2$ (r = 0.40), $P < 0.1$ (r = 0.50) and $P < 0.01$ (r = 0.70) significance levels.

Literature Cited in the Auxiliary Material

S1 Hansen MC, et al. (2003) Global Percent Tree Cover at a Spatial Resolution of 500 Meters: First Results of the MODIS Vegetation Continuous Fields Algorithm. *Earth Interact* 7:1–15.

S2 Sulla-Menashe D, et al. (2011) Hierarchical Mapping of Northern Eurasian Land Cover Using MODIS. *Remote Sens Env* 115:392-403.

S3 Zhou LM, et al. (2001) Variations in northern vegetation activity inferred from satellite data of vegetation index during 1981 to 1999. *J Geophys Res* 106:20069–20083.

S4 Sitch S, et al. (2003) Evaluation of ecosystem dynamics, plant geography and terrestrial carbon cycling in the LPJ dynamic vegetation model. *Glob Change Biol* 9:161–185.

S5 Kalnay E, et al. (1996) The NCEP/NCAR 40-Year Reanalysis Project. *Bull Amer Meteor Soc* 77:437–471.

S6 Harris, I., et al. (2013) Updated high-resolution grids of monthly climate observations – the CRU TS3.10 datase. *Int J Climatol* doi:10.1002/joc.3711.

S7 Giglio L, et al. (2013) Analysis of daily, monthly, and annual burned area using the fourth generation Global Fire Emissions Database (GFED4), *J Geophys Res* doi:10.1002/jgrg.20042..